JJMIE

Volume 20, Number 3, September 2026
ISSN 1995-6665
Pages 435– 446
https://doi.org/10.59038/jjmie/200309
Editor-in-Chief: Prof. Faris M. AL-Oqla

Jordan Journal of Mechanical and Industrial Engineering

Development and Performance Evaluation of a Solar-Powered Water Surface Cleaning Boat with Overloading Indicator

Firas Basim Ismail[1,2,3], Karam S. Khalid[4], Muhammad Imran Hasani[1], Rami H. Al-Hadeethi[5*], Ammar Al-Bazi[6]

[1]Smart Power Generation Research Centre, Institute of Power Engineering, Universiti Tenaga Nasional (UNITEN), Kajang, 43000, Malaysia.
[2]Faculty of Engineering, Sohar University, PO Box 44, Sohar PCI 311, Oman.
[3]Engineering College, Al-Bayan University, Baghdad, Iraq
[4]Aeronautical Technical Engineering Department, Technical Engineering College, AL-Farahidi University, 10070 Baghdad, Iraq.
[5]School of Engineering and Digital Technologies, Faculty of Management, Sciences and Engineering, University of Bradford, Bradford BD7 1DP, United Kingdom
[6]Operations and Service Management Department, Aston Business School, Birmingham, UK.

Received 15 Oct 2025 Accepted 9 May 2026

Abstract

To mitigate the growing threat of water pollution, water surface cleaning boats have been developed to collect floating solid waste. However, existing solar-powered systems often lack overload monitoring capabilities, which may lead to instability and operational risks. This study presents the development and performance evaluation of a photovoltaic-powered water surface cleaning boat equipped with an overloading indicator to enhance operational safety. The system was modeled using Creo Parametric 6.0 and analyzed in ANSYS to evaluate hydrodynamic drag and structural performance. Experimental validation was conducted to assess the boat's operational characteristics under different loading conditions. The results indicate that the system achieves up to 88.4% of the rated solar panel output under field-testing conditions, demonstrating effective energy utilization. The structural analysis yielded a factor of safety of 1.03, which is acceptable for prototype-level validation but requires further improvement for full-scale deployment. The proposed system integrates waste collection, solar energy utilization, and overload protection into a single platform. The findings confirm the feasibility of the developed prototype and highlight its potential for sustainable water surface cleaning applications, while also identifying areas for future structural enhancement.

Keywords: Solar-powered boat; Water surface cleaning; Photovoltaic systems; Experimental validation; Environmental sustainability.

1. Introduction

In recent years, there is a concerning lack of awareness regarding individual responsibilities to preserve the environment. Regrettably, many individuals exhibit a careless attitude when it comes to the disposal of food packaging and plastic waste, often seen discarding them thoughtlessly into bodies of water. Plastic bottles and even straws are thrown away after being used by humans as well[1-2]. The dry leaves from the trees, on the other hand, will fall onto the water's surface. Waste can be consumed by marine species such as fish and turtles, causing them serious disease or death. These factors contribute to severe water pollution that will become toxic to the environment and humans [3]. By considering the water's condition, trash collector boats have been invented to clean up bodies of water on regular basis[4-5]. In order to remove waste items and floating sediments from waterways, the majority of them are built with several functions, such as a hydrocarbon separator and a scraper[6]. At the end of the process, the accumulated trash will be thrown into the allocated trash can[7]. Due to the high concentration of pollutants in water bodies, manual cleaning is not a proper measure and may be harmful and detrimental to the operator [8-9].

Additionally, water surface cleaning boats have been equipped with solar photovoltaics (PV) to ensure continued performance. In the modern world, solar energy has become one of the most popular kinds of energy and a widely embraced renewable energy source [10-11]. Solar energy generation has several unique characteristics, the most notable of which are renewable resources and low maintenance costs. The system is straightforward to assemble and maintain, and it can be rapidly and silently deployed. There are no harmful emissions or damaging substances [12-13]. Solar energy will primarily power the boat's motor, providing for practically limitless recreation as long as solar energy is available. Because solar energy will not always be sufficient to power the motor due to the

* Corresponding author e-mail: r.h.f.al-hadeethi@bradford.ac.uk.

sun being regularly blocked by clouds, limiting the effectiveness of solar PVs, rechargeable batteries are needed as a backup, particularly at night[14].

Under the current solar PV-powered water surface cleaning boats, the development of this boat has several benefits, including being environmentally friendly and being able to recover the boat's dying energy source by alternating the solar panel and the battery. Unfortunately, the currently used designs have a number of drawbacks, including a lengthy operation period (if the solar panel is the main power source) and an inability to alert the user if the external loads transferred onto the boat have reached or exceeded the maximum load the boat can sustain. If the user does not take this issue seriously, the boat's efficiency will be compromised, and the boat may sink.

Some research lacks adequate analysis, such as hull drag analysis, stress-strain analysis, and material selection for product manufacture. Most studies don't examine product performance to see whether it's optimal. On the basis of the issues stated in the problem statement, the project's scope of work entails the development and evaluation of a new design for better boat movement, as well as the monitoring and control of the boat's performance after its fabrication to verify its quality and verifiability. In this research, the deliverables of the project will be specified and listed.

On top of that, the aim of this study is to develop and evaluate an ideal design of a PV-solar-powered water surface cleaning boat capable of alerting the user when the gathered floating trash has reached or surpassed the boat's maximum capacity.

Although several studies have reported solar-powered or remotely operated water surface cleaning boats, many existing prototypes focus primarily on conceptual demonstrations without comprehensive structural verification, numerical analysis, or systematic experimental validation. In particular, limited attention has been given to operational safety during garbage collection, such as warning mechanisms to prevent overloading and unintended sinking. Furthermore, several reported designs lack quantitative performance assessment under real environmental conditions. In this context, the present study focuses on the development and experimental validation of a laboratory-scale functional prototype, emphasizing dimensional design, component integration, structural verification, and real-world performance testing. Rather than pursuing full naval architectural optimization, this work aims to evaluate practical feasibility by integrating a solar photovoltaic system, a battery backup, and a simple overloading indicator, followed by systematic experimental assessment. The novelty of this work lies in the combined implementation of an overloading warning mechanism with solar-assisted operation and in the validation of performance parameters through numerical simulations and multi-day experimental testing on an actual water body.

This study presents the development and experimental validation of a photovoltaic-powered autonomous water surface cleaning system, with emphasis on practical feasibility and operational safety. A load-dependent performance framework is established to relate buoyancy behavior, propulsion characteristics, and energy consumption under varying operating conditions. The system integrates a hybrid photovoltaic–battery energy architecture to ensure continuous operation despite fluctuations in solar irradiance. In addition, a real-time load monitoring and warning mechanism is developed to prevent overloading and minimize the risk of instability during garbage collection. The proposed design and control approach are validated through numerical simulations and multi-day experimental testing under realistic environmental conditions, demonstrating the reliability and applicability of the system for sustainable water surface cleaning operations.

2. Materials and Methods

This section will provide a full explanation of the methods used. Proper parameter calculation, drawing, and 3D design analysis using Creo Parametric are included to determine the design specifications and material analysis. After implementation, performance testing is carried out to evaluate the system's performance.

2.1. Design Methodology

The best design for the boat will be determined in this phase, as well as product design parameters and the design optimisation process for the selected PV-operated water surface cleaning boat. In addition, a 3D model of the major pieces and a completely constructed boat will be shown, together with an isometric view layout for dimensioning purposes using Creo Parametric 6.0 software. The boat's critical elements that will be subjected to stress will be assessed by a von Mises stress-strain analysis combined with a safety factor to guarantee that the parts are within the permissible limit to preserve the boat's performance. The safety factor can be calculated using Equation (1) below [15]:

$$S_f = \frac{S_y}{\sigma_{max}} \quad (1)$$

Where the factor of safety (FoS) represents the ratio between the material yield strength and the induced stress. The yield strength refers to the maximum stress the material can withstand before failure, while the induced stress corresponds to the von Mises stress obtained from the structural analysis. This parameter is used to evaluate the structural reliability of the boat under loading conditions.

ANSYS software is used to do a hull drag analysis to determine the structural entity of the boat. The software can simulate the flow around a hull and is suitable for boat design [16]. The materials analysis will be undertaken as part of the verification process to move this project forward to the next step.

Before settling on product design specifications, a theoretical calculation of design parameters are considered as an initial planning step before beginning product manufacture. Some examples of design parameters necessary for this product are the speed, mass transfer rate, and torque generated by the conveyor. The modification on the boat will be explained in more detail to overcome the research gap. Simply put, when the boat is collecting a large amount of floating waste and pass it to its storage compartment, the portion of the boat's body that is submerged in the water will increase, and the water level at the water level sensor will also rise. After a specific level has been set to signify that the boat is overloading, same will happen to the buzzer will be operated to alert the user to clear the storage area before using the boat again.

Structural and hydrodynamic analyses were performed using Creo Parametric 6.0 and ANSYS software to evaluate stress distribution and flow interaction, respectively. For the structural analysis, the boat body material was modeled as polystyrene with a yield strength of 34 MPa. A static load corresponding to the maximum experimental payload was applied, and a von Mises stress criterion was employed.

For the hydrodynamic analysis, a steady-state flow condition was assumed. The water velocity was set to 1.0 m/s, while the surrounding air velocity was set to 3.0 m/s to represent mild environmental conditions. The computational domain was discretized using a tetrahedral mesh, with mesh refinement applied near the hull surface. These assumptions are consistent with low-speed, small-scale prototype operation and are sufficient for comparative performance evaluation.

The computational domain was discretized using a fine mesh to ensure accurate flow prediction around the hull. A steady-state solver was employed with a velocity inlet boundary condition and pressure outlet condition. The hull surface was defined as a no-slip wall. These conditions simulate realistic operating conditions of the boat moving through water at low speed.

The boat dimensions were selected based on buoyancy and stability considerations derived from the prototype development. The total weight of the system, including structural components, battery, conveyor system, and solar panel, was estimated and compared with the buoyant force generated by the displaced water volume. The design ensures that the buoyant force exceeds the total system weight, thereby maintaining floatation stability. Additionally, the center of gravity was kept low by placing heavier components such as the battery at the base of the structure to enhance stability during operation.

The stability of the boat was qualitatively evaluated by ensuring a balanced weight distribution and symmetric hull configuration. The twin-hull (catamaran) design improves lateral stability and reduces the risk of overturning. This configuration increases the metacentric height, contributing to better equilibrium when subjected to external disturbances such as water currents and uneven loading conditions.

2.2. Theoretical design parameters formula

There will be five main parameters that are required for this product, which are the speed of the boat, mass transfer rate, torque generated by the conveyor of the boat, charging time and the solar power harvested. Each of these parameters will be discussed in detail later on. The speed of the boat will be one of the most important parameters that need to be included, as the speed will also determine the effectiveness of the product. The speed of the boat and thrust force can be determined by using equations(2–5)[17].

$$\text{Power Required} = \text{Current} \times \text{Voltage} \tag{2}$$

Where the brake shaft power (BSP) represents the power required to drive the propeller and overcome the resistance acting on the boat during motion.Where brake shaft power (BSP) = power required.

$$\text{Propeller Velocity (VP)} = \text{rotational speed of propeller} \times 0.514 \times 0.9 \tag{3}$$

Where thrust force is the force generated by the propeller to propel the boat forward, and it depends on the power delivered to the propeller and the efficiency of the propulsion system.

$$\text{Thrust Force } (T) = \frac{\text{Effective Power (EP)}}{\text{Propeller Velocity (VP)}} \tag{4}$$

where the efficiency represents the effectiveness of the propulsion system in converting input power into useful thrust, accounting for energy losses. Speed of the boat [18]:

$$\text{Boat speed } (v) = \frac{\text{Thrust Force } (T) \times \text{time } (t)}{\text{mass } (m)} + \text{Initial speed } (u) \tag{5}$$

Where the speed of the boat is defined as the distance travelled per unit time, and it is influenced by the thrust force, hydrodynamic resistance, and total load acting on the boat.

The transfer rate of the conveyor is one of the important parameters that need to be considered to ensure the effectiveness of the boat in collecting solid floating garbage. The solid floating garbage mainly consists of plastic-based materials and lightweight wood. The standard speed for the dual-axis gear is 90 rpm (which is around 9.43 m/s), and the material's mass on a one-meter conveyor is 0.00016 kg/m. Hence, the transfer rate for the conveyor to transfer the floating garbage into the storage area within one second can be calculated using Equation 6.

$$T = 3.6MS \tag{6}$$

Where the mass transfer rate represents the amount of floating waste transported by the conveyor per unit time. It depends on the conveyor speed and the mass of material per unit length, indicating the effectiveness of the collection mechanism. Mass transfer rate at the conveyor[19].The torque generated by the conveyor is also important to find out the effectiveness of the conveyor that is moved by the motors during its operation. The torque generated can be ascertained after finding out the requirement from equations (7) and (8) as below. Power requirement for the conveyor [20]:

$$\text{Mass} = \frac{QL\lambda}{367} + \frac{DL}{20} \tag{7}$$

Where the power requirement refers to the energy needed to operate the conveyor system, which depends on the load being transported and the conveyor speed. The torque generated by the conveyor [20]:

$$Torque = \frac{60 \times 1000 \times P \times \eta}{2 \times \pi \times N} \tag{8}$$

Where torque is the rotational force generated by the motor to drive the conveyor. It is directly related to the power supplied and the angular velocity of the system.

The rechargeable batteries will be connected with the 6 V 4.5 W and 750 mA solar panel. For the rechargeable batteries' specifications, the batteries are 18650 model with 3.7 V 2000 mAh. There will be two rechargeable batteries connected in series; hence, the current value will be the same. The total charging time for these batteries can be calculated from equation (9)below. The boat design, and specifications are shown in Table 1.Rechargeable battery charging time [21]:

$$\text{Charging Time} = \frac{\text{Battery Current Capacity}}{\text{Solar Panel Current}} \tag{9}$$

Where the charging time represents the duration required to fully charge the batteries. It depends on the battery capacity and the charging current supplied by the solar panel.

The overall system efficiency was evaluated based on the ratio of useful electrical output power to the total solar energy input. The system achieved approximately 88.4% utilization of the rated solar panel power under experimental conditions, indicating effective energy conversion and minimal losses within the system.

Table 1. Initial product design specifications

Parameters	Details	Remark
Length	37.5 cm	-
Width	30.0 cm	-
Height	21.5 cm	-
Product weight	1 kg	Depends on the materials
Performance parameters		
Initial operation speed	0.024 m/s	Without load
Final operation speed	0.008 m/s	Fully loaded
Maximum load capacity	6 kg	-
Operational range	300 m	Radius from the user
Mass transfer rate	1.533 g/s	Can vary
Torque generated	3.8765 N·m	Generated from conveyor
Charging time	2.67 hours	-
Safety requirement		
Factor of safety	1.5	Fully-assembled design
Electronics protection	Divider	Prevent water leakage
Hydraulic analysis		
Water flow	Steady one-dimensional flow	No reverse flow in the channel

The solar panel rating was selected based on the system power requirements obtained from the propulsion motor and conveyor mechanism. The total power demand was estimated from the motor specifications, and a 6 V, 4.5 W solar panel was selected to provide sufficient energy under standard sunlight conditions. The battery acts as an energy storage unit to ensure continuous operation during fluctuations in solar irradiance.

2.3. Design and performancetestings implementation

After all the design parameters are stated, the fabrication process is done to build the prototype. Figure 1shows the finalised product.

After that, seven performance tests are implemented to monitor and observe the product's performance. The location of the tests is done in a lake in Universiti Tenaga Nasional (UNITEN), Malaysia, and any irregularities in data will show the anomalies in the experiment. After the results have been obtained, the graphs have been generated as an effective deliverable to present the results in the simplest form. The list of performance tests is shown below:

1. Float water level sensor calibration
2. Buzzer operating range
3. Storage area capacity
4. Boat speed and maximum operational distance
5. Power requirement and maximum power harvested
6. Product's operating limit and charging time
7. Mass transfer rate

The formula to determine the mass transfer rate can be observed from the equation(10) below[22]:

$$\text{Mass transfer rate} = \frac{(m_2 - m_1)}{(t_2 - t_1)} \quad (10)$$

Where the mass transfer rate is calculated based on the total mass of collected waste divided by the time taken for collection. This provides an experimental evaluation of the conveyor performance.

The speed of the boat can be determined from equation(11) below:

$$\text{Speed} = \frac{\text{Distance}}{\text{Time}} \quad (11)$$

Where the boat speed is determined by dividing the total distance travelled by the time taken. This parameter is used to assess the operational performance under different loading conditions.

The power harvested from the panel can be calculated by using equation (2). The AR Ruler's application is used to measure the distance between the user and the buzzer for buzzer operating range testing. This application consists of measurement applications that use the smartphone camera to measure an object [23].

In this final phase, all the results obtained are analysed and discussed thoroughly to justify and validate the product based on its performance and compare it with the already existing products. The proper graphs are generated depending on the parameters obtained from the testing. The conclusion can be made after all the experimental values for the design parameters are validated with the theoretical values and the product is proven to be more enhanced than the currently used systems.

The recorded data are compared with the theoretical values by applying the percentage difference formula as shown in equation (12) below[24]:

$$\text{Percentage difference} = \frac{|\,\text{Theoretical value} - \text{Experimental value}\,|}{\text{Theoretical value}} \times 100 \quad (12)$$

Where the percentage error represents the deviation between the experimental and theoretical values. It is used to evaluate the accuracy and reliability of the obtained results.

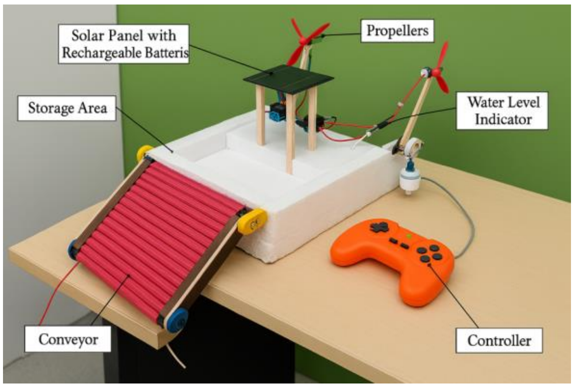

Figure 1. The fabricated prototype

Following the completion of the performance tests, the data has been analysed and discussed in further depth. The results of the tests are validated by comparing them with the theoretical values. A comparison table is made for the benchmarking to compare the product's performance with the existing products to ensure that the product is justified and validated to be more enhanced compared to the existing products.

2.4. Design Scope and Limitations of the Prototype

The design presented in this study corresponds to a functional prototype intended for experimental validation and performance assessment at a small scale. The dimensional parameters were selected to ensure adequate buoyancy, payload accommodation, and integration of mechanical and electrical components. The scope of the design does not include full naval architectural optimization, hydrostatic certification, or compliance with maritime classification standards. Instead, the emphasis is placed on structural feasibility, operational stability under low-speed conditions, and functional validation of the cleaning and warning systems. This scope is appropriate for evaluating practicality and identifying areas for future large-scale design improvements.

3. Results and Discussions

3.1. Design assessment of solar-powered water-cleaning boat

After all of the essential parts have been modelled using Creo software, the parts have been fabricated, and assembled accordingly, which will be identical to the preliminary sketch. The fully assembled product's 3D modelling can be shown in Figure 2.

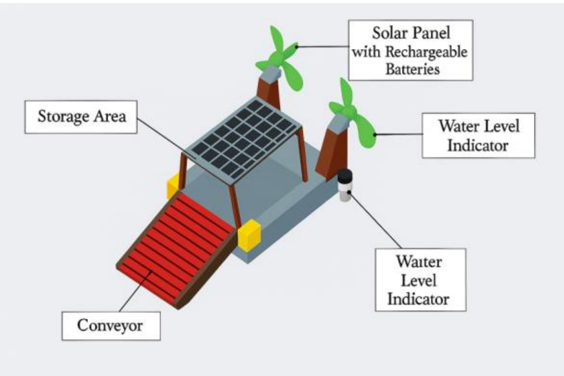

Figure 2. Fully-assembled design in Creo software

The final design of the boat has been analysed for the factor of safety as the boat's body, which will carry the load, and the obtained factor of safety is obtained using Creo Parametric 6.0 and von Mises stress-strain analysis [25-26]. The yield strength of the boat's main part, which is thermocol (polystyrene), is ascertained to be 34 MPa. The von Mises stress is obtained from the simulation result with 32.9 MPa.

The stress distribution obtained from the numerical simulation reveals non-uniform stress behavior across the structure. Higher stress concentrations are observed at critical regions, particularly around the propeller support columns, shaft interfaces, and the front ramp connection, where load transfer and geometric discontinuities occur. In contrast, the main hull and upper frame experience relatively low stress levels, indicating effective load distribution throughout the structure. The simulated stress values range from approximately 0.08 MPa to 32.82 MPa, as illustrated in Figure 3, and remain within the allowable limits of the selected material. These results confirm the structural adequacy and integrity of the proposed surface water cleaning boat design under the applied loading conditions.

The structural analysis resulted in a calculated factor of safety of 1.03 under the maximum considered loading condition, as determined using Eq. (1). This value indicates a marginal safety margin, which is acceptable for a laboratory-scale prototype operating at low speed and low load in controlled freshwater environments. However, this factor of safety is lower than typical engineering design recommendations for full-scale or commercial marine structures. The obtained result highlights the importance of future design enhancements, including the use of alternative materials, increased hull thickness, or structural reinforcement, to achieve a minimum factor of safety of 1.5 or higher for long-term deployment. In the context of this study, the calculated safety factor is sufficient to demonstrate functional feasibility while clearly identifying structural limitations for future work. The material yield strength, maximum von Mises stress, and corresponding safety factor values are summarized in Table 2.

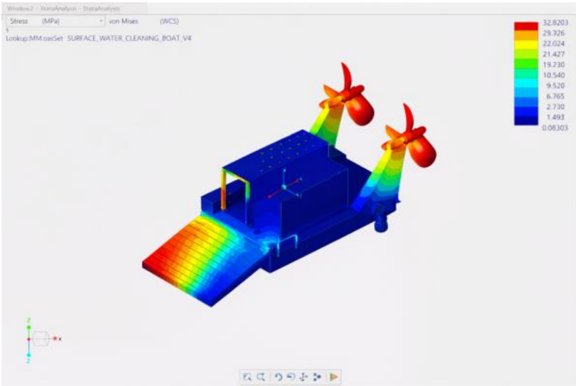

Figure 3. Stress-strain analysis in Creo software

Table 2. Safety factor of the design

Yield strength (MPa)	Von mises stress (MPa)	Safety factor
34	32.9	1.03

The experimental tests were conducted under controlled conditions and repeated multiple times to ensure consistency. The collected data were averaged to minimize random measurement errors. The results demonstrate good agreement with the theoretical predictions, confirming the validity of the proposed design. Static stability was assessed experimentally by observing the relationship between applied load and submerged depth. Results showed a monotonic increase in submerged depth with increasing payload, without sudden instability or capsize during testing. The maximum allowable submerged depth was established at 4 cm, above which an overloading condition was detected by the warning system. Throughout experimental operation under maximum allowable load, the prototype maintained upright orientation and stable motion, indicating adequate static stability for low-speed water surface operation.

The hull drag analysis determines the boat's watertight enclosure in operation [27]. Another operating parameter to consider is the water flow, which should be a stable one-dimensional flow and not a reversible flow in the channel since it may impair the boat's performance. In one-dimensional flow (no different direction of the stream water), air velocity is 3.0 m/s, and the water velocity is 1.0 m/s. Another goal of this research is to identify the boat's structure to guarantee its stability in the water. This includes the boat's water and air friction. The whole boat design cannot be analysed. Hence, the main body has been chosen for the test.

From the obtained results in Figure 4, it can be seen that the boat is in a stable position, and the velocity obtained during the simulation also shows that it is acceptable, as the velocity is not too high nor too low, which is within the acceptable range velocity of the boats.

3.2. Experimental Validation Setup

The developed photovoltaic-powered water surface cleaning system was experimentally validated under real operating conditions. The prototype was deployed in a controlled water environment to assess its performance in terms of propulsion, waste collection efficiency, and operational stability. The system consists of a floating platform integrated with a conveyor-based waste collection mechanism, powered by a photovoltaic (PV) panel and battery storage system. During testing, different loading conditions were applied to evaluate system response and performance degradation under increasing waste accumulation. Key performance parameters measured include propulsion capability, conveyor efficiency, mass transfer rate, and power consumption. The experimental procedure involved repeated trials under varying load conditions to ensure consistency and reliability of results.

Figure 5 illustrates the prototype during real-time operation, highlighting the floating structure, conveyor system, and photovoltaic module. Additional observations were made to evaluate system stability and efficiency under practical environmental conditions.

Figure 5. Experimental validation of the developed photovoltaic-powered water surface cleaning boat during field testing, showing active collection of floating debris under real lake environment.

3.3. Testing of output performance

In this section, all the results obtained from the performance testing are analysed and discussed in more detail to justify and validate the product's performance. In addition, the obtained results are validated by comparing the experimental results with the theoretical values. Experimental measurements were subject to uncertainties arising from environmental disturbances, instrument accuracy, and observation limitations. Repeated tests were conducted over multiple days to ensure consistency of results. The overall uncertainty in measurements is estimated to be within ±5–10%, which is acceptable for this type of field-based engineering system. To minimize random error, key experiments were repeated over four days and average values were considered. Despite these uncertainties, the observed trends were consistent, supporting the reliability of the reported results. Error bars were not included due to limited repeatability resolution; however, repeated experiments over four days produced consistent trends.

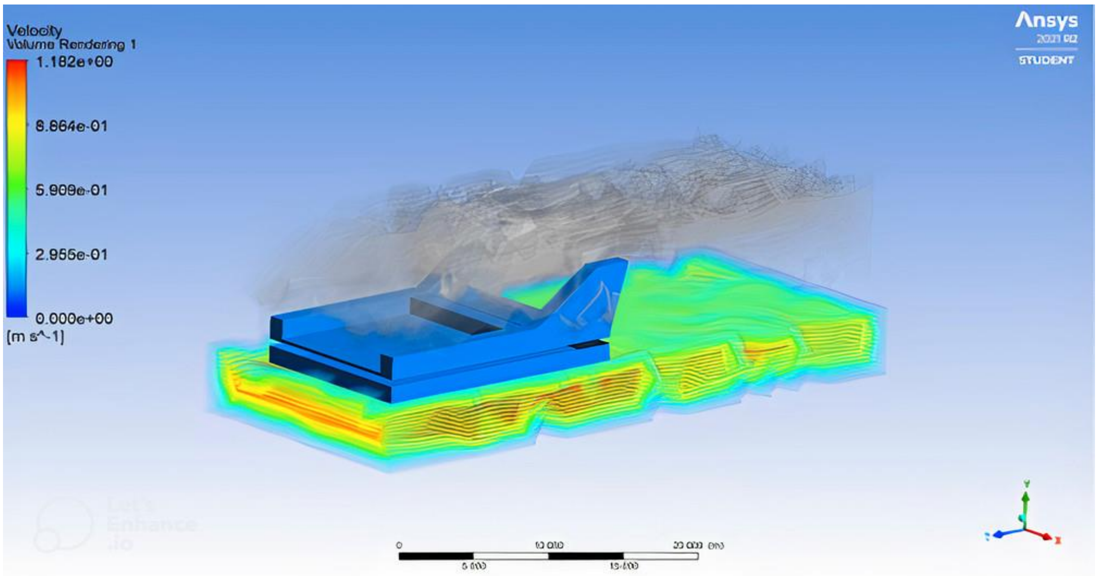

Figure 4. Hull drag analysis in Ansys software

3.3.1. Water Level Sensor Calibration Testing

After implementing the float water level sensor testing, the depth of the boat's body that submerged into the water is recorded until the buzzer is activated to determine the maximum depth that the boat can withstand. There is a scale mark at the boat's side for depth reference before putting the boat onto the water for testing (refer to prototype in Figure 1).

Table 3. Float water level sensor calibration testing's result

Depth submerged (cm)	Buzzer status (on/off)
0	off
1	off
2	off
3	off
4	on

From the obtained results, the maximum depth that the boat can withstand is 4 cm deep, and it cannot submerge beyond that level. This result is significant as the boat's submerged depth will be applied at the storage area capacity testing later on.

3.3.2. Buzzer Operating Range Testing

For the buzzer's performance testing, the boat will travel through different distances, and the sound of the buzzer will be recorded until the user cannot hear the buzzer's sound to find out how far the user can hear the buzzing during the boat's operation. The distance of the user with the buzzer is determined using the AR Ruler's application, and Table 4 shows the results of the testing:

Table 4. Buzzer operating range testing's result

Distance travelled from the user (m)	Buzzer's sound availability (yes/no)
20	yes
40	yes
60	yes
80	yes
100	yes
120	no

The reading will be stopped once the sound of the buzzer cannot be heard anymore, and the user stated that the sound of the buzzer was lost when the user was 120 m apart from the boat. It is safe to assume that the buzzer's maximum operational range is 100 m from the user; hence, the user needs to consider the distance between them to ensure that the user can hear the buzzer when the boat is overloaded. The standard operational range for the 6 V buzzer is 80 to 100 meters; hence, the buzzer's performance is within the acceptable range.

3.3.3. Storage Area Capacity Testing

Based on the obtained results from float water level sensor calibration testing, The utmost depth the boat can reach is 4 cm, and if the depth exceeds 4 cm due to overloading, the boat will overload. The mass of the load is recorded first by using the weighing scale. Figure 6 shows the graph of the load applied and depth submerged against the mass applied inside the storage area.

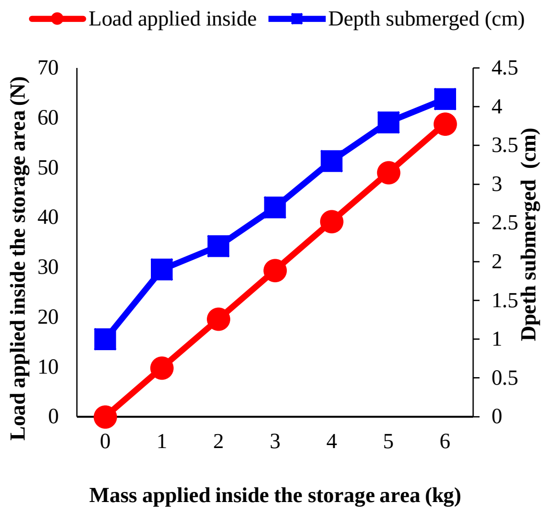

Figure 6. Relationship between the depth submerged and load applied against mass applied

From the obtained results, the depth submerged and load applied inside the storage area is directly proportional to the mass applied into the storage area of the boat, where the more garbage that enters the storage area, the more the boat's body will submerge into the water. As from the float water level sensor calibration testing, the maximum depth that the boat can reach is 4 cm, and the current result shows that the maximum weight that the boat can withstand is 50 N because, at 60 N, the boat has submerged until 4.1 cm which is exceeding the maximum depth for the boat to submerge.

The inconsistent graph may be caused by external factors such as parallax error or the weighting scale's systematic error during the data readings. This maximum capacity of the storage area is only an experimental value as the real weight that can be applied onto the boat is unreached because the boat can only pick up the miniature solid floating garbage such as leaves, plastic bottles and twigs.

3.3.4. Boat Speed and Maximum Operating Distance Testing

The test for boat speed is done for four days by using an application that can measure the distance of an object from a particular origin, which is the AR Ruler's application. There will be two different data for the distance travelled by the boat, which are the distance travelled by the boat without load and for the fully loaded (maximum load applied, which is 5 kg), as shown in Figure 7. There were readings of speed without load and others for fully loaded. Figure 7 shows the graph of the average speed and distance travelled against the time.

According to Figure7, the results show that the distance travelled is directly proportional to the time, but, the graph exhibits an irregular pattern that may be attributed to the wind-induced drag force or the wave generated during the experiment, both of which influence the boat's speed. For the maximum operating distance of the boat, it can be seen that the boat stopped moving after it travelled 160m away from the user. Hence, the maximum operating distance of the boat is 160 m. The slowness of the boat may be due to the low power generated by the DC motors (propellers), which reduce the thrust force to push the boat.

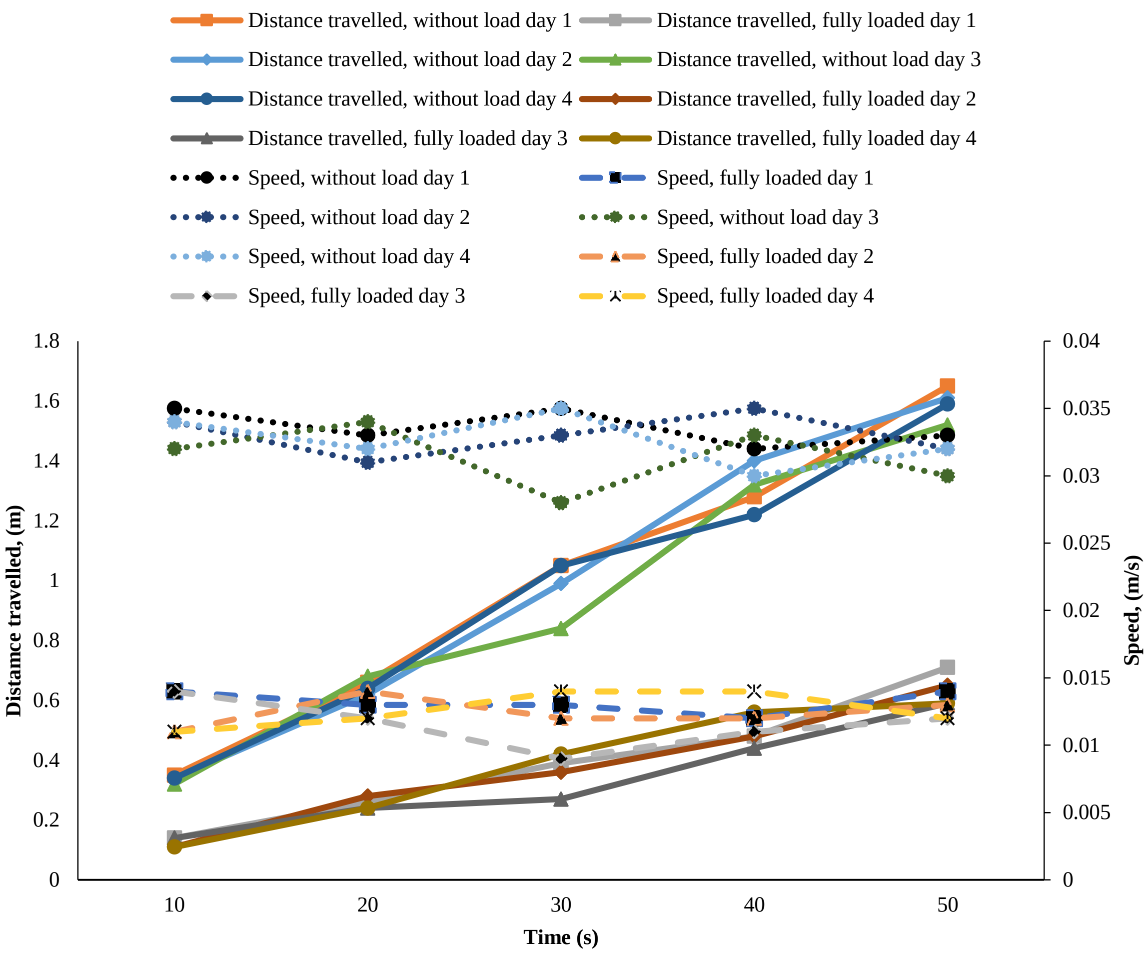

Figure 7. Graph of average speed against days of testing

3.3.5. Power Requirement and Maximum Power Harvested Testing

Four main parts require the power source to operate: the conveyor, propellers, controller, and the water level indicator system. Each of these parts will undergo power requirement testing by using the multimeter to determine the minimum power and voltage for all four parts to work. The power is calculated by multiplying the input voltage with the input current. Table 5 shows the result of the testing where the percentage error can be obtained by referring to equation (12), which involved the rated voltage and input voltage.

From the obtained result in Table 5, the total power requirement for the product to operate is 7.03 W. In order to validate the result, the percentage error has been taken into account for each of the necessary parts, and all the percentage errors calculated are within the acceptable range where all the percentages are below 20 %. The power requirement is one of the most important features in the product design specifications. By comparing two different products with different power consumption, the lower power consumption product will be selected as it is cheaper than the power supply purchased for the higher power consumption product.

For the maximum power harvested by the solar panel, the output voltage and output current values are calculated to find out the power harvested. The percentage of output power gained is obtained, and Figure 8 shows the results of the power-harvested testing.

Table 5. Power requirement testing's result

Part	Input voltage (V)	Rated voltage (V)	Input current (A)	Input power (W)	Percentage error (%)
Propellers	5.78	6	0.352	2.03	3.67
Conveyor	5.23	6	0.391	2.04	12.83
Controller	2.88	3	0.244	0.70	4.00
Water level indicator	5.86	6	0.385	2.26	2.33

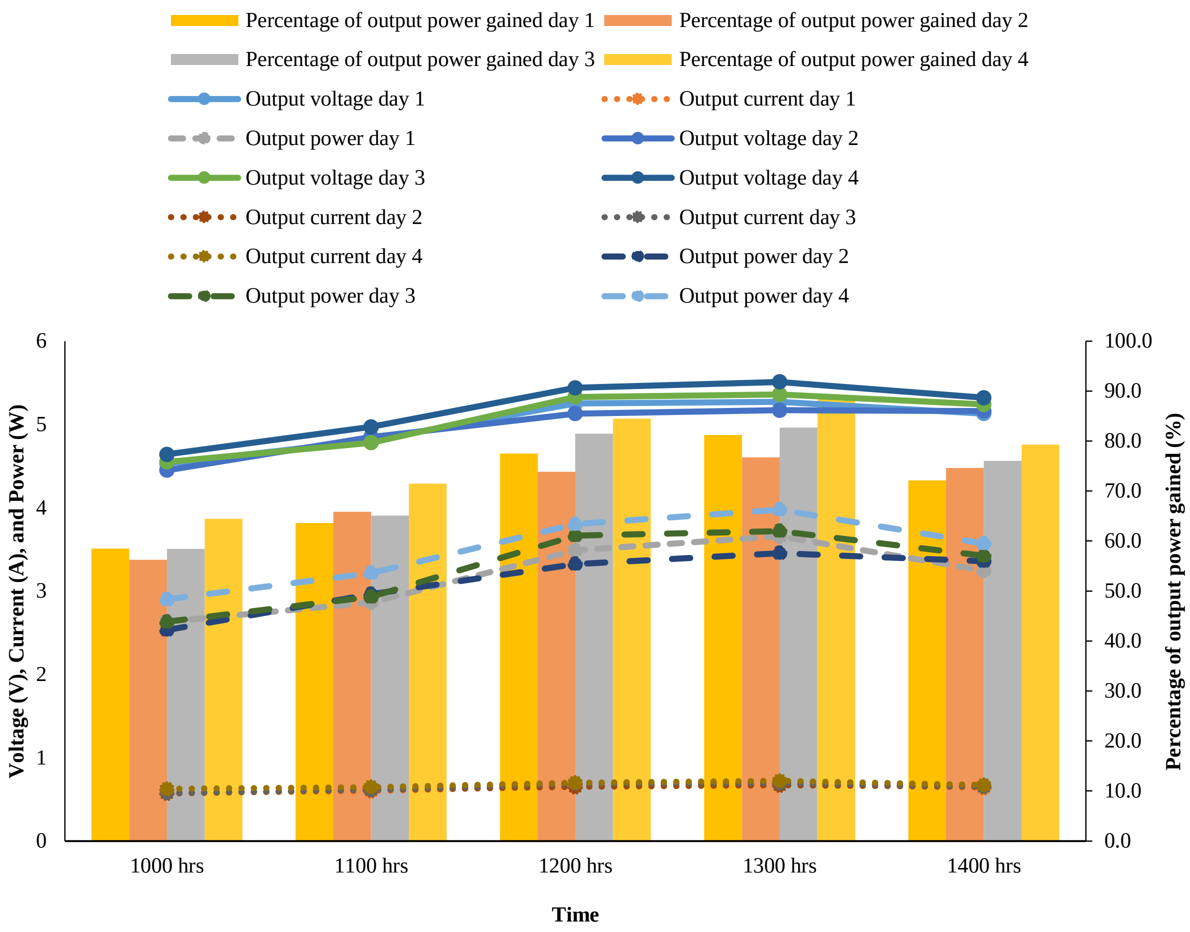

Figure 8. Graph of power harvested, current, voltage and percentage error against time.

It can be seen that the maximum power that the solar panel can harvest is at 1:00 p.m., and the maximum power harvested is calculated as 3.98 W on day 4 with a percentage of output power produced at 88.4 %. The results reveal that by measuring the percentage of output power acquired on the solar PV panel, the performance of the panel displays a consistent pattern throughout the four-day tests. As a result, the performance of the solar PV panel is evaluated and justified.

The solar energy system consists of a 6 V, 4.5 W monocrystalline photovoltaic panel coupled with two 3.7 V, 2000 mAh rechargeable lithium-ion batteries connected in series. The solar panel primarily supplies power to the conveyor system, while the batteries provide backup power for propulsion and control components. This hybrid configuration ensures continuous operation under varying solar irradiation conditions, including partial cloud cover and low-light periods.

3.3.6. Maximum Operating Time and Charging Time Testing

The only part that will be connected to the solar PV system is the conveyor; hence, the other parts will use the batteries as the power source to operate. Even though the conveyor will be using solar energy, all the parts will undergo testing to make sure that the boat will not stop when it reaches the time limit during the cleaning operation later. This testing will determine how long each part can work until the batteries die, and the duration (subtracting the ending time from the starting time) will be recorded. The maximum ending time is 11:00 a.m. on Wednesday, but if the selected parts stop working at a particular time, it will be recorded as the ending time in Table 6.

Table 6. Maximum operating time testing result

Part	Starting time	Ending time	Operating duration
Propellers	11:00 a.m. (Monday)	6:09 p.m. (Monday)	7 hours and 09 minutes
Conveyor	11:00 a.m. (Monday)	5:14 p.m. (Monday)	6 hours and 14 minutes
Controller	11:00 a.m. (Monday)	11:00 a.m. (Wednesday)	48 hours
Water level indicator	11:00 a.m. (Monday)	11:00 a.m. (Wednesday)	48 hours

Based on the obtained result, the lowest operating duration is the conveyor; hence, after 6 hours and 14 minutes, the boat needs to return to the user to replace the original batteries with the new ones, the boat cannot perform well and will lead to poor performance (such as incapability to collect the garbage). In addition, if the boat suddenly stops during its operation, the boat might stay in the middle of the lake, and the user will have difficulties getting the boat back. The testing is implemented at the same starting time for the rechargeable batteries charging time. The time taken for the batteries to be fully charged can be observed in Table 7 below.

Table 7. Charging time testing's result

Day	Starting time	Ending time	Charging duration
1	11:00 a.m.	2:10 p.m.	3 hours and 10 minutes
2	11:00 a.m.	1:40 p.m.	2 hours and 40 minutes
3	11:00 a.m.	2:23 p.m.	3 hours and 23 minutes
4	11:00 a.m.	1:55 p.m.	2 hours and 55 minutes

Based on the theoretical calculation for the charging time, the time taken for the 18650 rechargeable batteries to be fully charged by the 4.5 W solar panel is 2 hours and 40 minutes, and the average charging time from this testing is 3 hours and 4 minutes hence the performance for this particular part is acceptable. The charging time deviates slightly from the theoretical value due to weather and measurements accuracy.

3.3.7. Mass Transfer Rate Testing

The mass transfer rate is showing how fast the conveyor can transfer the solid floating garbage into the storage area, depending on the capability of the conveyor to withstand the loads. By applying the trip method, the boat will travel along a trip estimated at around 20 metres, and the travel time and mass of the garbage collected will be recorded. Five trips have beenimplemented for four daysto ascertain the consistency of the data, and the average mass transfer rate is calculated. The travel time for the distance of 20 metres has been recorded from 4 to 5 minutes. Figure 9 portrays the graph of the mass transfer rate and total mass inside storage area for the whole four days.

Based on the obtained results in Figure 9, the pattern shows the irregularity in the mass inside storage area and mass transfer rate that may be due to the availability of the floating leaves and the slider's capability to collect the floating garbage. This may be contirbuted to the depression angle of the slider. The depression angle needs to be increased to enhance the conveyor's transfer rate. In addition, some of the garbage did not float on the water's surface but sank instead. The next reason is that the boat's speed is quite slow, which may be due to the generation of opposite force from the conveyor that reduces the net force of the boat. It can be seen that the boat is moving very slowly, which affects the boat's performance in collecting the floating garbage.

In order to improve the performance of this mass transfer rate, the boat needs to increase its depression angle so that the boat can collect the floating garbage more effectively. The speed of the boat can also be boosted by changing the propellers to bigger-sized propellers to create greater thrust force and, will increase the speed of the boat. Even though the mass transfer rate of the conveyor is low, the result shows that the experimental value is better than the theoretical value, where the theoretical value is 5.508 kg/hr while the average experimental value 5.616 kg/hr. Hence, it is confirmed that the conveyor can operate well to collect the garbage as the mass transfer rate has been validated with the theoretical value.

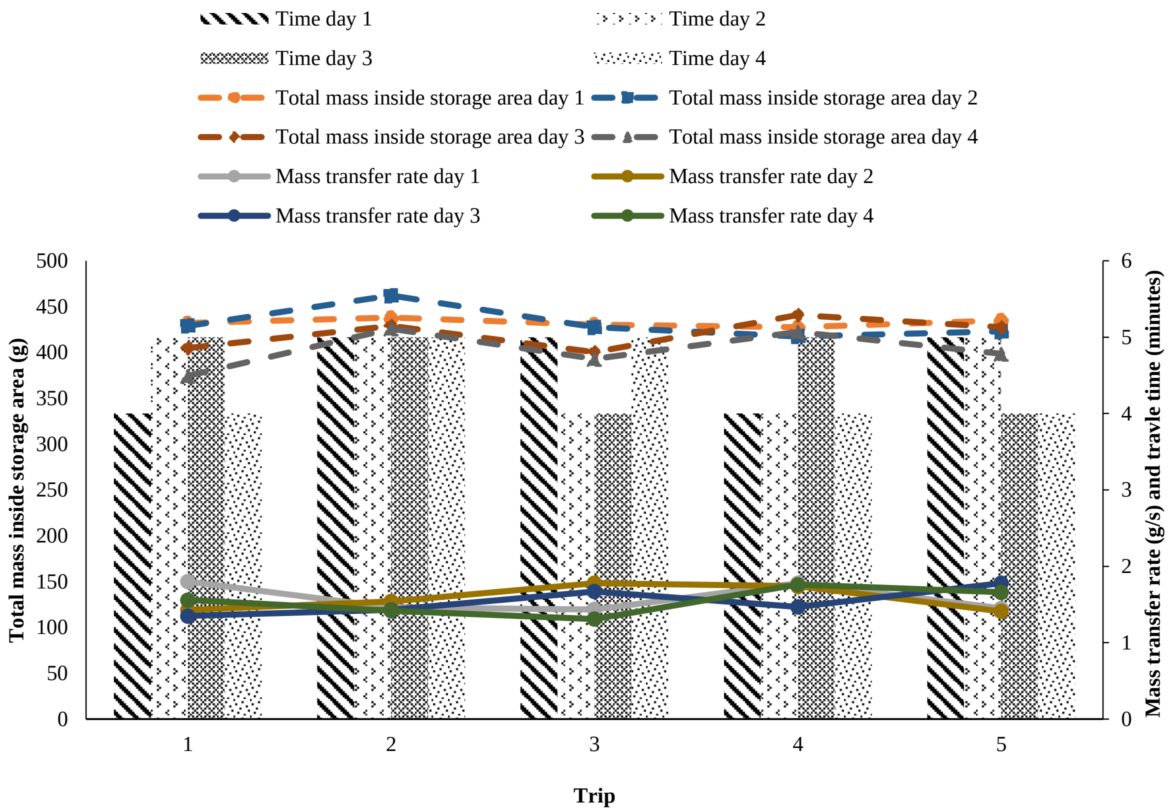

Figure 9. Graph of mass transfer rate with total mass inside storage area and travel time against trip

3.4. Summary of Performance Testing Results

As Table 1 only provides theoretical product design specifications for validation and verification, the detailed product design specifications are depicted in Table 8, with values derived from previous performance testing in Section 3.2. The finalised product design specifications can be observed in Table 8 below. The percentage error of the parameters between theoretical and experimental values is calculated using equation (12).

Table 8. Comparison of finalised product design specifications with theoretical values

Specification	Description		
	Theoretical	Experimental	Percentage error (%)
Weight	1 kg	0.95 kg	5.0
Maximum load capacity	60 N	49 N	18.3
Power requirement	7 W	7 W	0.0
Operational speed	0.024 m/s	0.035 m/s	45.8
Operational duration	-	6 hours and 14 minutes	-
Operating range	300 m	160 m	47
Mass transfer rate	1.53 g/s	1.56 g/s	2
Propeller controlling	Radio control	Radio control	-
Conveyor controlling	Relay (switch)	Relay (switch)	-
Buzzer operational range	-	100 m	
Maximum power harvested by solar panel	4.5 W	3.702 W	17.8
Rechargeable batteries charging time	2 hours and 40 minutes	3 hours and 4 minutes	-
Additional feature	Overloading indicator and solar PV system	Overloading indicator and solar PV system	-

All these parameters obtained from the performance tests are verified and validated successfully with the theoretical values with the percentage error within the acceptable range. The tests are repeated for four days, and the average value is considered to ensure minimum experimental error.

The energy performance of the system was evaluated by comparing the maximum electrical power harvested from the solar panel with its rated capacity. Experimental results showed a peak output power of 3.98 W at approximately 13:00 hours, corresponding to 88.4% of the rated panel power. This indicates effective utilization of available solar irradiation under field conditions.

When compared with the total system power requirement of approximately 7 W, the solar panel was able to supply a significant portion of the operational energy, with the remainder provided by the battery system. These results demonstrate that the prototype achieves a satisfactory level of energy efficiency for a small-scale solar-assisted cleaning boat. Compared with previous studies on water surface cleaning systems [4,5], the present work integrates solar energy utilization and an overloading protection mechanism, which enhances both operational efficiency and system safety. While earlier designs focused mainly on mechanical collection, this study provides a more comprehensive approach by combining structural, hydrodynamic, and energy performance evaluation.

3.5. Model Validation and Error Analysis

A comparison between theoretical predictions and experimental measurements is presented in Table 8. The results indicate good agreement, with percentage errors of approximately 2% for mass transfer rate, 0% for power requirement, and 18.3% for load capacity. The observed discrepancies are primarily attributed to environmental disturbances such as wind-induced drag, surface wave effects, and minor inconsistencies in waste distribution during testing. Additionally, measurement limitations and sensor accuracy contribute to the deviation. Overall, the results confirm that the proposed analytical model provides a reliable estimation of system performance under practical operating conditions.

4. Conclusion

This study presented a development and experimental validation of a solar-powered water surface cleaning boat prototype equipped with an overloading indicator. Structural and hydrodynamic analyses were conducted using Creo Parametric and ANSYS, followed by multi-day experimental testing in a real water body. The prototype demonstrated stable operation at low speed, with a maximum allowable load of 49 N and a maximum operating distance of 160 m. Experimental results showed that the solar photovoltaic system achieved a peak output of 3.98 W, corresponding to 88.4% of its rated power, while the overall system power requirement was approximately 7 W. The overloading indicator effectively alerted the user when the maximum safe submerged depth was reached. Although the calculated factor of safety was marginal, it was sufficient for prototype-level validation and highlighted areas for future structural improvement. The findings confirm the feasibility of integrating solar energy and safety features into a water surface cleaning boat. Future work will focus on structural reinforcement, efficiency enhancement, improved propulsion, and weather-proof electronic enclosures to enable large-scale and long-term deployment. Despite the promising results, the system is limited by a relatively low factor of safety and small-scale testing conditions. Future work should focus on structural reinforcement and full-scale validation under real environmental conditions.

Declaration of interest statement

"We the authors declare no affiliations with or involvement in any organization or entity with any financial interest (such as honoraria; educational grants; participation in speakers' bureaus; membership, employment, consultancies, stock ownership, or other equity interest; and expert testimony or patent licensing arrangements), or non-financial interest (such as personal or professional relationships, affiliations, knowledge or beliefs) in the subject matter or materials discussed in this manuscript".

Conflict of Interests

"The authors declare that there is no conflict of interests regarding the publication of this article".

Data Availability

"The research data is available upon request. To request the data, contact the first author of the article".

Acknowledgements

The authors acknowledge the support provided by Universiti Tenaga Nasional (UNITEN), Malaysia, during the experimental testing of the prototype.

References

[1] Prabhu, S. M., Irshad, M. K., Rahman, M., and Shahil, M., "Design and fabrication of river cleaning machine" *International Research Journal of Engineering and Technology*, vol. 6, no. 7, pp. 225–232, 2019.https://www.irjet.net/archives/V6/i7/IRJET-V6I739.pdf

[2] Hua, A. K., "Analytical and detection sources of pollution based on environmetric techniques in Malacca River, Malaysia," *Applied Ecology and Environmental Research*, vol. 15, no. 1, pp. 485–499, 2017.https://www.aloki.hu/pdf/1501_485499.pdf

[3] Gupta, A., and Singh, M. R., *Water Pollution: Sources, Effects and Control*, New Delhi: APH Publishing Corporation, 2014.

[4] Abdullah, S. H. Y. S., Azizudin, M. A. A., and Endut, A., "Design and prototype development of a portable trash collector boat for small stream application," *International Journal of Innovative Technology and Exploring Engineering*, vol. 8, no. 10, pp. 350–356, 2019.https://doi.org/10.35940/ijitee.I8291.0881019

[5] Raj, B. S., Murali, L., Vijayaparamesh, B., Kumar, J. S., and Pragadeesh, P., "IoT-based water surface cleaning and quality checking boat," *Journal of Physics: Conference Series*, vol. 1937, 2021.https://doi.org/10.1088/1742-6596/1937/1/012023

[6] Tang, Y. Y., Tang, K. H. D., Maharjan, A. K., Aziz, A. A., and Bunrith, S., "Malaysia moving towards sustainable municipal solid waste management," *Industrial and Domestic Waste Management*, vol. 1, no. 1, pp. 26–40, 2021.https://doi.org/10.53623/idwm.v1i1.51

[7]S. S. Hegde, S. Shetty, P. Shah, and S. Shastri, "Design of an autonomous water cleaning bot," Materials Today: Proceedings, vol. 46, pp. 8742–8747, 2021.https://doi.org/10.1016/j.matpr.2021.04.044

[8] Zhu, J., Yang, Y., and Cheng, Y., "SMURF: A fully autonomous water surface cleaning robot with a novel coverage path planning method," *Journal of Marine Science and Engineering*, vol. 10, no. 11, 2022.https://doi.org/10.3390/jmse10111620

[9]N. A. S. Kamarudin, I. N. A. MohdNordin, D. Misman, and N. Khamis, "Development of Water Surface Mobile Garbage Collector Robot," Alinteri Journal of Agriculture Sciences, vol. 36, no. 1, pp. 534–540, 2021.https://doi.org/10.47059/alinteri/V36I1/AJAS21076

[10]Ishak, M. A. A. B., Ibrahim, A., Sopian, K., Fauzan, M. F., Rahmat, A. A., and Yusaidi, N. J. B., "Performance and economic analysis of a bifacial PVT solar collector," *International Journal of Renewable Energy Development*, vol. 12, no. 4, pp. 780–788, 2023.https://doi.org/10.14710/ijred.2023.54348

[11] Belsky, A. A., Glukhanich, D. Y., Carrizosa, M. J., and Starshaia, V. V., "Analysis of specifications of solar photovoltaic panels," *Renewable and Sustainable Energy Reviews*, vol. 159, 2022.https://doi.org/10.1016/j.rser.2022.112239

[12] Obaideen, K., et al., "On the contribution of solar energy to sustainable development goals: Case study on Mohammed bin Rashid Al Maktoum Solar Park," *International Journal of Thermofluids*, vol. 12, 2021.https://doi.org/10.1016/j.ijft.2021.100123

[13] Alghamdi, A. S., Bahaj, A. S., and Wu, Y., "Assessment of large-scale photovoltaic power generation from carport canopies," *Energies*, vol. 10, no. 5, pp. 686, 2017. https://doi.org/10.3390/en10050686

[14]Green, M. A., Dunlop, E. D., Hohl-Ebinger, J., Yoshita, M., Kopidakis, N., Bothe, K., Hinken, D., Rauer, M., Hao, X. "Solar cell efficiency tables (Version 60)," *Progress in Photovoltaics*, vol. 30, no. 7, pp. 687–701, 2022. https://doi.org/10.1002/pip.3595

[15] Rabie, N. A., Akl, S. A., and Hussien, A. K., "Effect of parameter uncertainty on factor of safety calculations in a slope stability problem," in *Proc. Geo-Congress*, ASCE, pp. 1842–1849, 2015.https://doi.org/10.1061/9780784479087.168

[16] Yousefi, R., Shafaghat, R., and Shakeri, M., "Hydrodynamic analysis techniques for planing hulls," *Applied Ocean Research*, vol. 42, pp. 105–113, 2013. https://doi.org/10.1016/j.apor.2013.05.004

[17] Molland, A. F., Turnock, S. R., and Hudson, D. A., *Ship Resistance and Propulsion*, Cambridge University Press, 2011.https://assets.cambridge.org/97805217/60522/frontmatter/9780521760522_frontmatter.pdf

[18] Koçak, M. B., and Barlas, B., "Investigation of boat motion on occupant in patrol boats," *Journal of Naval Sciences and Engineering*, vol. 17, no. 2, pp. 377–393, 2021. https://izlik.org/JA62EB96TC

[20] D. Mondal, "Consume Power Torque and Conveyor energy efficiency for a Horizontal Screw Conveyor with three different Screw Flight – A Comparison," 2021.

[19] Zhang, S., Xia, X."Optimal control of operation efficiency of belt conveyor systems," *Applied Energy*, 2010, pp. 1929-1937.http://doi.org/10.1016/j.apenergy.2010.01.006

[21]Ponrouch, A., Bitenc, J., Dominko, R., Lindahl, N., Johansson, P., &Palacín, M. R. "Multivalent rechargeable batteries," *Energy Storage Materials*, vol. 20, pp. 253–262, 2019.https://doi.org/10.1016/j.ensm.2019.04.012

[22] Gu, Z. H., Arnold, P. C., and McLean, A. G., "Prediction of flowrate of bulk solids from mass flow bins," *Powder Technology*, vol. 72, no. 2, pp. 157–166, 1992. https://doi.org/10.1016/0032-5910(92)88022-A

[23] Ching, E. T. Y., On, C. K., Alfred, R., Hijazi, M. H. A., Guan T. T. "An Android Mobile-based Measurement Application – Object and Interior Room Measurement App" *International Journal of Interactive Mobile Technologies*, vol. 14, no. 20, pp. 135–152, 2020.https://doi.org/10.3991/ijim.v14i20.15415

[24] Atkinson, G., and Batterham, A. M., "The use of ratios and percentage changes in sports medicine," *Sports Medicine*, vol. 51, no. 1, pp. 1–9, 2021. http://doi.org/10.1055/s-0032-1316355

[25]Griffiths, D. V., and Lane, P. A., "Slope stability analysis by finite elements," Géotechnique, vol. 49, no. 3, pp. 387–403, 1999. https://doi.org/10.1680/geot.1999.49.3.387

[26]Hughes, T. J. R., Cottrell, J. A., and Bazilevs, Y.,"Isogeometric analysis: CAD, finite elements, NURBS, exact geometry and mesh refinement,"Computer Methods in Applied Mechanics and Engineering, vol. 194, no. 39–41, pp. 4135–4195, 2005.https://doi.org/10.1016/j.cma.2004.10.008

[27] Wulandari, A. I., Sulisetyono, A., and Utama, I. K. A. P., "CFD Analysis into the Breakdown of Catamaran Resistance Based on the Original Formula by Insel and Molland" *CFD Letters*, vol. 17, no. 5, pp. 103–119, 2025.https://doi.org/10.37934/cfdl.17.5.103119